

OPTIMUM ROTOR PERFORMANCE IN AXIAL FLOW BY FINITE-STATE METHODS

by

David A. Peters
dap@me.wustl.edu

McDonnell Douglas Professor of Engineering
Chairman, Department of Mechanical and Aerospace Engineering

Cristina Garcia-Duffy
cgd@me.wustl.edu
Graduate Research Assistant

Washington University in Saint Louis
St. Louis, Missouri

Abstract

Recent studies have pointed out that conventional lifting rotors in forward flight have efficiencies far lower than the optimum efficiencies predicted by theory. Finite-state inflow models have been suggested as a theoretical basis whereby to study the reasons for this efficiency deficit. In this paper, a finite-state inflow model is utilized to formulate the optimum circulation and inflow distribution for rotors in axial flow. The results show that a formal optimization with finite-state models can be done in closed form and that such an optimization recovers the classical uniform-flow condition (for an actuator disk with an infinite number of blades), the Prandtl solution (for an actuator disk with a finite number of blades), the Betz distribution (for a lifting rotor with an infinite number of blades) and the Goldstein solution (for a lifting rotor with a finite number of blades). Thus, it should be possible to use finite-state models to investigate optimum rotor performance in forward flight.

Notation

$[A_{nj}^m]$	special case of the matrix \tilde{L}	$\bar{\bar{L}}$	\tilde{L} -matrix with the elements where $m = 0$ are multiplied by two
C_n^m, D_n^m	Fourier expansion coefficients for the pressure	m, r	harmonic number
C_p	power coefficient	P_I	induced power
C_{P_I}	induced power coefficient	P_s	shaft power
C_T	thrust coefficient	P_n^m	associated Legendre function of the first kind
$[E_{nj}^{m0}]$	expansion transformation matrix	\bar{P}_n^m	normalized associated Legendre function of the first kind
H	rotor inplane force	ΔP	rotor disk pressure
$[I]$	identity matrix	Q	power or number of blades
j, n	polynomial number	Q_n^m	associated Legendre function of the second kind
k	Prandtl's tip loss correction factor	\bar{r}	non-dimensional radial position
K	thrust deficiency	R	radius
K_n^m	kinetic energy matrix	t	time
L_q	blade loading	\bar{t}	$= \Omega t$
\tilde{L}^c, \tilde{L}^s	cosine and sine parts for the L-matrix	T	thrust
		u	horizontal component of induced velocity
		U	inplane flow
		v	vertical component of induced velocity
		V	flow normal to the disk
		V_∞	free-stream velocity
		w	induced flow
		W	inflow
		x	distance on the blade from the center of the rotor
		X	$= \tan \chi/2 $

Presented at the American Helicopter Society 63rd Annual Forum, Virginia Beach, VA, May 1-3, 2007. Copyright © 2007 by the American Helicopter Society International, Inc. All rights reserved.

α_n^m, β_n^m	induced flow expansion coefficients
η	climb rate = $v / \Omega R$
$\bar{\eta}$	ellipsoidal coordinate system component
θ	pitch angle
κ	swirl parameter = 2.2
λ	total inflow = $\eta + v$
Λ	Lagrange's multiplier
μ	advance ratio = $u / \Omega R$
v	ellipsoidal coordinate or $\sqrt{1 - r^2}$
\bar{v}	normalized inflow = $w / \Omega R$
ρ	density
τ_n^{mc}, τ_n^{ms}	pressure coefficients for Fourier series expansion
ϕ	angle between the lift and the thrust
ϕ_n^m	radial expansion shape function
Φ	pressure
χ	skew angle
ψ	angular position from rotor aft
$\bar{\psi}$	ellipsoidal coordinate
Ω	angular velocity

Introduction

Work-Energy principles indicate that the induced power P_I generated for a lifting rotor (i.e., the power that does not perform useful work) can be found by computing the shaft power and then subtracting the work done on the vehicle

$$P_I = P_S - TV - HU \quad (1)$$

where T is the thrust perpendicular to the disk, V is the rotor velocity in the T direction, H is the rotor force in the inplane direction, and U is the rotor velocity in the H direction (See Figures 1 and 2). By necessity, the magnitude of this power must equal the power that is expended into the kinetic energy of the induced flow. It follows that simple, Glauert momentum theory can be used to compute the minimum possible induced power for a given flight condition. Based on these, one would predict that a rotating wing in forward flight would be almost as efficient as a fixed-wing aircraft. However, flight test data (as well as comprehensive simulations) give induced power several times as large as the ideal value. In an effort to determine the source of those deficiencies, Ormiston [1],[2] performed extensive runs with RCAS to try to determine why the actual results were differing from the ideal results. In these studies, the profile drag of the airfoil was assumed to be zero so that the induced power could be separated. The results of those studies similarly showed that there is an order-of-magnitude difference between ideal induced power and

the actual induced power of rotorcraft. An obvious question is, "Why is there such a difference?"

Several potential sources of decreased efficiency can be identified in terms of the physics of an actual rotor as compared to an ideal actuator disk. First, an ideal disk produces thrust perpendicular to the disk whereas a true rotor produces a tilted thrust vector that results in swirl velocity. Therefore, there is lost energy. Second, an ideal rotor has an infinite number of blades whereas a true rotor has a discrete number. The fact that there are vortex sheets coming off the individual blades implies an upwash outside of the slipstream that further translates into lost energy. Third, an ideal disk can generate an arbitrary lift distribution over the span and azimuth. An actual blade, on the other hand, can only produce lift under the constraints of both allowable blade pitch changes and of the limits on airfoil lift coefficients at high angles of attack. The ultimate goal of the present research effort is to determine which of these contribute to the drastic increase in induced power and, consequently, what changes in rotor hardware (if any) might address the issue.

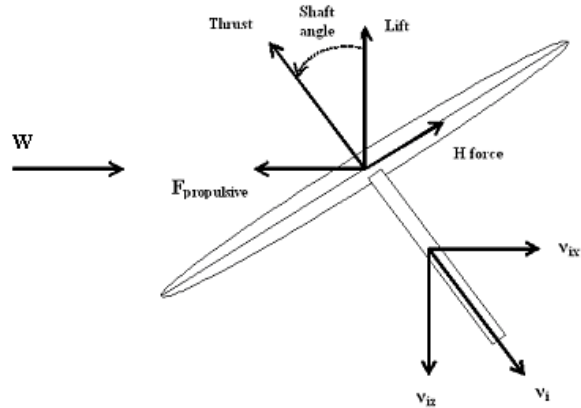


Figure 1: Basic illustrative problem for a rotor [1].

The scope of such a study is so broad that the use of large, comprehensive codes is prohibitive for these purposes. On the other hand, finite-state wake models are ideally suited to such task. These models expand both the pressure field and the velocity field in orthogonal expansion functions. Therefore, the computation of induced power (the dot product of thrust and induced flow) simplifies nicely into a quadratic cost function that allows classical optimization to be used for the minimum power under a variety of constraints. Thus, it is anticipated that such an approach can yield insight into this issue. As a preliminary step in such an endeavor, this present paper looks at the induced power of a non-ideal lifting rotor in axial flow to verify that dynamic wake models can indeed compute the proper induced power.

Since theory and experiment agree with simple momentum approaches for power in axial flow, such conditions provide the ideal test bed to verify that this optimization approach is viable. Future studies will then concentrate on induced power in forward flight.

Optimization with Finite-State Model

He inflow equations.

He [3] developed an unsteady induced-flow theory to be used in stability, vibration, control, and aeroelastic studies. The theory is based on an acceleration potential for an actuator disk. The induced flow, w , is expressed in a polynomial distribution (proportional to Legendre functions) radially and in terms of a Fourier series azimuthally. The way the induced flow is set up allows for all harmonics and describes the induced flow for any radial position.

The He theory provides the pressures on the rotor disk as a Fourier expansion. As more harmonics are added, that pressure converges to the lift concentrations on the blade and to zero lift off the blade. One of the issues to be addressed in this present work is whether or not such an approach can give adequate convergence to induced power. The form of this pressure expansion is as follows:

$$\Phi(v, \bar{\eta}, \bar{\psi}, \bar{t}) = \rho \Omega^2 R^2 \sum_{m=0}^{\infty} \sum_{n=m+1, m+3, \dots}^{\infty} P_n^m(v) Q_n^m(i\bar{\eta}) \cdot [C_n^m(\bar{t}) \cos(m\bar{\psi}) + D_n^m \sin(m\bar{\psi})] \quad (2)$$

The pressure at the rotor disk is obtained by the difference between the pressure above and the pressure below the disk.

$$\Delta P(\bar{r}, \psi, t) = \rho \Omega^2 R^2 \sum_{m=0}^{\infty} \sum_{n=m+1, m+3, \dots}^{\infty} \bar{P}_n^m(v) \cdot [\tau_n^{mc}(\bar{t}) \cos(m\psi) + \tau_n^{ms}(\bar{t}) \sin(m\psi)] \quad (3)$$

The power Q can be expressed as:

$$Q = \iint_A \Delta P(w+v) x dx d\psi \quad (4)$$

The He model also sets out the velocity field normal to the rotor disk in terms of the same Legendre Functions and variables, as given below.

$$w(\bar{r}, \psi, \bar{t}) = \Omega R \sum_{m=0}^{\infty} \sum_{n=m+1, m+3, \dots}^{\infty} \phi_n^m(\bar{r}) \cdot [\alpha_n^m(\bar{t}) \cos(m\psi) + \beta_n^m(\bar{t}) \sin(m\psi)] \quad (5)$$

$$\phi_n^m(\bar{r}) \equiv \frac{1}{v} \bar{P}_n^m(v) \quad (6)$$

where $\bar{t} = \Omega t$, and $\phi_n^m(\bar{r})$ are a complete set of functions that arise from the solution to Laplace's equation in ellipsoidal coordinates.

The form of the functions is:

$$\phi_n^m(\bar{r}) = \sqrt{(2n+1)H_n^m} \sum_{q=m, m+2, \dots}^{\infty} \bar{r}^q \frac{(-1)^{(q-m)/2} (n+q)!!}{(q-m)!!(q+m)!!(n-q-1)!!} \quad (7)$$

$$\text{where } H_n^m = \frac{(n+m-1)!!(n-m-1)!!}{(n+m)!!(n-m)!!}$$

substitution of the induced flow and the pressure at the disk yields:

$$Q = \rho \Omega^3 R^5 \sum_{m,n} \int_0^1 \int_0^{2\pi} \left[\lambda + \sum_{r,j} \frac{1}{v} \bar{P}_j^r(v) \cdot (\alpha_j^r \cos(r\psi) + \beta_j^r \sin(r\psi)) \right] \cdot [\bar{P}_n^m(v) (\tau_n^{mc} \cos(m\psi) + \tau_n^{ms} \sin(m\psi))] v dv d\psi \quad (8)$$

$$Q = 2\pi \rho \Omega^3 R^5 \int_0^1 \sum_n \left[\lambda + \sum_j \phi_j^0 \alpha_j^0 \right] \bar{P}_n^0 \tau_n^{0c} v dv + \pi \rho \Omega^3 R^5 \int_0^1 \sum_{m,n} \left\{ [\phi_j^m \alpha_j^m] \bar{P}_n^m \tau_n^{mc} + [\phi_j^m \beta_j^m] \bar{P}_n^m \tau_n^{ms} \right\} v dv \quad (9)$$

The functions P_n^m are Legendre Functions of the first kind, and v is related to the radial position by $r = \sqrt{1-v^2}$.

The equations that relate the pressure coefficients in the pressure expansion $(\tau_n^{mc}, \tau_n^{ms})$ to the velocity coefficients (α_j^r, β_j^r) are derived from the momentum equation of potential flow.

$$[K_n^m] \{ \dot{\alpha}_n^m \} + V [\tilde{L}^c]^{-1} \{ \alpha_n^m \} = \frac{1}{2} \{ \tau_n^{mc} \} \quad (10)$$

$$[K_n^m] \{ \dot{\beta}_n^m \} + V [\tilde{L}^s]^{-1} \{ \beta_n^m \} = \frac{1}{2} \{ \tau_n^{ms} \} \quad (11)$$

where $(\dot{}) = \frac{d}{dt}$, $V = \frac{\mu^2 + (\lambda + v)\lambda}{\sqrt{\mu^2 + \lambda^2}}$, λ is the total inflow,

μ is the advance ratio, V is the flow parameter, and K_n^m is diagonal; $K_n^m = \frac{2}{\pi} H_n^m$. The $[\tilde{L}]$ cosine and sine matrices are given in closed form in terms of the wake skew angle, χ .

$$\Gamma_{jn}^{rm} = \frac{(-1)^{\frac{n+j-2r}{2}}}{\sqrt{H_n^m H_j^r}} \frac{2\sqrt{(2n+1)(2j+1)}}{(j+n)(j+n+2)[(j-n)^2-1]}$$

for $r + m$ even

$$\Gamma_{jn}^{rm} = \frac{\pi}{2\sqrt{H_n^m H_j^r}} \frac{\text{sgn}(r-m)}{\sqrt{(2n+1)(2j+1)}}$$

for $r + m$ odd, $j=n\pm 1$

$$\Gamma_{jn}^{rm} = 0$$

for $r + m$ odd, $j \neq n\pm 1$

(12)

$$\begin{aligned} [\tilde{L}_{jn}^{0m}]^c &= X^m \Gamma_{jn}^{0m} \\ [\tilde{L}_{jn}^{rm}]^c &= [X^{|m-r|} + (-1)^l X^{|m-r|}] \Gamma_{jn}^{rm} \\ [\tilde{L}_{jn}^{rm}]^s &= [X^{|m-r|} - (-1)^l X^{|m-r|}] \Gamma_{jn}^{rm} \end{aligned}$$

(13)

where $l = \min(r,m)$, $X = \tan|\chi/2|$. The forcing functions, τ_n^m , are given in terms of the blade loading, L_q .

$$\begin{aligned} \tau_n^{0c} &= \frac{1}{2\pi} \sum_{q=1}^Q \left[\int_0^1 \frac{L_q}{\rho \Omega^2 R^3} \phi_n^0(\bar{r}) d\bar{r} \right] \\ \tau_n^{mc} &= \frac{1}{\pi} \sum_{q=1}^Q \left[\int_0^1 \frac{L_q}{\rho \Omega^2 R^3} \phi_n^m(\bar{r}) d\bar{r} \right] \cos(m\psi_q) \\ \tau_n^{ms} &= \frac{1}{\pi} \sum_{q=1}^Q \left[\int_0^1 \frac{L_q}{\rho \Omega^2 R^3} \phi_n^m(\bar{r}) d\bar{r} \right] \sin(m\psi_q) \end{aligned}$$

(14)

Theorem on Induced Power.

A Rotor Induced-Power Theorem is used to verify the approach of this work. Let a rotor, Figure 2, be moving along an arbitrary, straight path through still air with a velocity W . Let χ be the angle between the flight path and a vertical to the rotor.

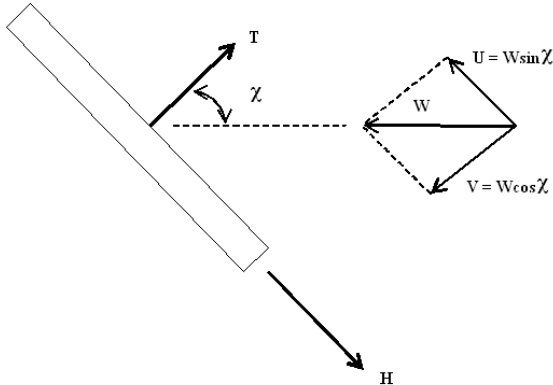


Figure 2: Inflow velocity components for a moving rotor.

It follows that the inplane component of air velocity as seen by the rotor is $U = W \sin \chi$ and the normal component is $V = W \cos \chi$.

Let the rotor loading perpendicular to rotor plane be called T and the rotor load in plane be called H , each with a positive sense in the direction of the flight path (i.e., opposite to V and U). Let the blades in the rotor disk be rotating counter-clockwise at angular velocity Ω , when looking down on the rotor, and let ψ be the azimuth angle of a blade as measured from aft, $\psi = \Omega t$. Let a generic point on the blade be a radial distance x from the center of rotation as shown on Figure 3.

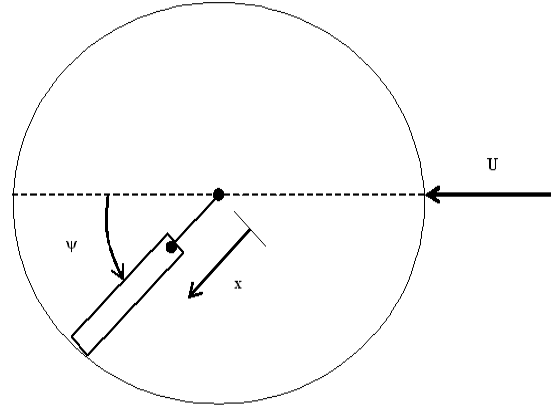


Figure 3: Rotor blade generic position and rotating angle.

Let ϕ be the inflow angle as seen in the local blade system, Figures 3 and 4. In that system, let dL be the incremental local lift per unit length (perpendicular to the total inflow), let dD be the incremental local induced drag per unit length, and let dT be the incremental thrust. Let w be the induced flow, opposite to L , Figure 4.

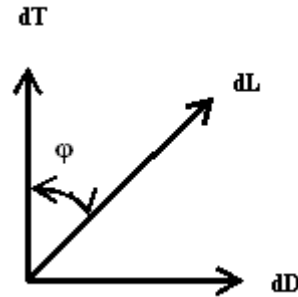


Figure 4: Geometry of the forces on the blade.

$$dT = dL \cos \phi \quad (15)$$

$$dD = dL \sin \phi \quad (16)$$

$$dH = -dD \sin \psi \quad (17)$$

Figure 5, taken from the work of Glauert [4], shows the geometry of the flow in the blade coordinate system. The relative flow due to rotor motion alone is $\Omega x + U \sin(\psi)$ in the rotor plane and V perpendicular to that plane. The induced flow w must be parallel to the lift, so

it is added vectorally at the angle ϕ as shown (see Glauert). The resultant total inflow (due to rotor motion and due to induced flow) must be perpendicular to the local incremental lift, due to circulation considerations. Therefore, w can be considered perpendicular to the total flow vector. The resultant relationships gives rise to the geometry in the figure and to the following identities:

$$\tan \phi = \frac{w \cos \phi + V}{\Omega x - w \sin \phi + U \sin \psi} = \frac{V + \frac{w}{\cos \phi}}{\Omega x + U \sin \psi} \quad (18)$$

$$\sin \phi = \tan \phi \cos \phi = \frac{V \cos \phi + w}{\Omega x + U \sin \psi} \quad (19)$$

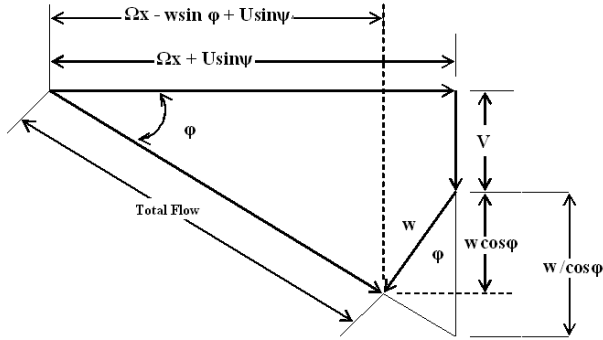


Figure 5: Geometry of the flow.

The above can be used to transform the induced power equations.

$$P_i = P_s - TV - HU \quad (1)$$

$$P_i = L \Omega x \sin \phi - L \cos \phi V + L \sin \phi \sin \psi U \quad (20)$$

$$P_i = L(\Omega x + U \sin \psi) \sin \phi - L \cos \phi V \quad (21)$$

(where the differentials are omitted for clarity).

But $\sin \phi = \frac{V \cos \phi + w}{\Omega x + U \sin \psi}$. Therefore

$$P_i = LV \cos \phi + Lw - LV \cos \phi = Lw \quad (22)$$

The induced power is, then:

$$\boxed{P_i = Lw} \quad (\text{work done by } L \text{ on } w) \quad (23)$$

Thus, the incremental induced power can be found from the integral of the dot product of the local lift and local induced flow, which is the work done on the flow field. The above theorem is, strictly-speaking, exactly true only for axial flow because of the assumption that local lift is parallel to local induced flow. On the other hand, that assumption is less and less important as one transitions away from hover. Furthermore, it is exactly true that the work done on the flow field will equal the induced power. Therefore, Equation (23) seems a valid approach to computing the induced power from a dynamic wake model.

Induced power derivation from He model.

For the Peters-He model in its actuator-disk form, we have a skewed wake as shown in Figure 6 below.

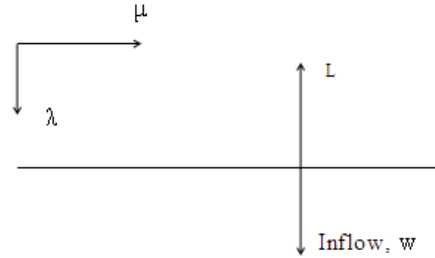


Figure 6: Normalized velocity components.

The power Q can be found from Equation (4) to be:

$$Q = \iint_A \Delta P (w + v) x dx d\psi$$

Notice that the power does not depend on the velocity component u . The pressure at the disk (as shown in equation (3)) is:

$$\Delta P = \rho \Omega^2 R^2 \sum_{m,n} \bar{P}_n^m(v) [\tau_n^{mc} \cos(m\psi) + \tau_n^{ms} \sin(m\psi)]$$

$$\text{Advance ratio } \mu = \frac{U}{\Omega R} \quad (24)$$

$$\text{Climb rate } \lambda = \frac{V}{\Omega R} \quad (25)$$

$$\text{Non-dimensional radial position } \bar{r} = \frac{x}{R} \quad (26)$$

$$\text{Non-dimensional inflow } \bar{v} = \frac{w}{\Omega R} \quad (27)$$

Note that $r dr = -v dv$, and λ and μ are constant.

The inflow is given by Equation (5).

Introducing the definitions for pressure change, v from the climb rate, and the induced velocity we obtain the expression for the power where the climb rate, λ , is a

constant. The normalized Legendre function is $\bar{P}_1^0 = \sqrt{3}v$ by definition. Introduction of it into the expression for the power yields Equation (28). By the use of the simple relationship between power and power coefficient, we obtain the following,

$$Q = 2\pi\rho\Omega^3 R^5 \int_0^1 \sum_n \left[\lambda + \sum_j \frac{1}{v} \bar{P}_j^0 \alpha_j^0 \right] \bar{P}_n^0 \tau_n^{0c} v dv + \pi\rho\Omega^3 R^5 \int_0^1 \sum_{m,n} \sum_j \left\{ \left[\frac{1}{v} \bar{P}_j^m \alpha_j^m \right] \bar{P}_n^m \tau_n^{mc} + \left[\frac{1}{v} \bar{P}_j^m \beta_j^m \right] \bar{P}_n^m \tau_n^{ms} \right\} v dv \quad (28)$$

$$C_p = \frac{Q}{\pi\rho\Omega^3 R^5} = 2 \left(\frac{\lambda}{\sqrt{3}} + \alpha_1^0 \right) \tau_1^{0c} + 2 \sum_{n=3,5,\dots} \alpha_n^0 \tau_n^{0c} + \sum_{m=1,2,3,\dots} \sum_{j=m+1,m+3,\dots} \left[\alpha_j^m \tau_j^{mc} + \beta_j^m \tau_j^{ms} \right] \quad (29)$$

and

$$C_T = 2 \left\{ \tau_n^m \right\}^T \left\{ C_n^m \right\} \quad (30)$$

A simple check using $m = 0$ only, and $n = 1$ only, provides the common expression that shows the Peters-He model agrees with the induced power from Momentum Theory. The lift and pressure coefficients for this special case are shown in equations (31) through (33).

$$\alpha_1^0 = \frac{1}{\sqrt{3}} \bar{v} \quad (31)$$

$$\tau_1^{0c} = \frac{\sqrt{3}}{2} C_T \quad (32)$$

$$C_p = \frac{2}{\sqrt{3}} (\lambda + \bar{v}) \frac{\sqrt{3}}{2} C_T = C_T (\lambda + \bar{v}) \quad (33)$$

Equations (29) and (30) provide the framework for a classical, quadratic optimization of power.

Optimization.

The classical quadratic optimization problem is stated as follows:

Minimize $\{x\}^T [A]\{x\}$ subject to $\{c\}^T \{x\} = q$ (given).

Use of Lagrange's multiplier to include the constraint leads to the cost function.

$$J = \frac{1}{2} \{x\}^T [A]\{x\} - \Lambda \{c\}^T \{x\} \quad (34)$$

where Λ is the Lagrange multiplier. Optimizing, we obtain that for the change of the functional to be zero

$$\delta J = \{\delta x\}^T \left[\frac{1}{2} [A + A^T] \{x\} - \Lambda \{c\} \right] = 0 \quad (35)$$

$$\{x\} = \left[\frac{1}{2} ([A] + [A]^T) \right]^{-1} \{c\} \Lambda \quad (36)$$

Notice that the matrix to be inverted is the symmetric part of $[A]$.

The Lagrange multiplier must be chosen such that:

$$\Lambda = \frac{q}{2\{c\}^T \left[\frac{1}{2} ([A] + [A]^T) \right]^{-1} \{c\}} \quad (37)$$

We may now apply this approach to the case for minimum induced power that we are presently discussing. For an actuator disk, with infinite number of blades that is lightly loaded, we will minimize C_p for a given C_T .

$$C_p = \sum_{n=1,3,5,\dots} 2\alpha_n^0 \tau_n^{0c} + \sum_{m=1,2,\dots} \sum_{n=m+1,m+3,\dots} \alpha_n^m \tau_n^{mc} \quad (38)$$

$$C_T = 2 \left\{ \tau_n^m \right\}^T \left\{ C_n^m \right\} \quad (39)$$

Physically, the coefficients C_n^m are a Legendre-function fit to the function $v \cos \varphi$ and they are defined as:

$$C_n^0 = \frac{1}{2\pi} \int_0^{2\pi} \int_0^1 \cos \varphi \bar{P}_n^0(v) v dv d\psi \quad (40)$$

$$C_n^{mc} = \frac{1}{2\pi} \int_0^{2\pi} \int_0^1 \cos \varphi \bar{P}_n^m(v) v dv \cos(m\psi) d\psi \quad (41)$$

$$C_n^{ms} = \frac{1}{2\pi} \int_0^{2\pi} \int_0^1 \cos \varphi \bar{P}_n^m(v) v dv \sin(m\psi) d\psi \quad (42)$$

where

$$\cos \varphi = \frac{r + \mu \sin \psi}{\sqrt{(r + \mu \sin \psi)^2 + \lambda^2}} \quad (43)$$

Then, the relationship between the coefficients and the function $\cos \varphi$ becomes:

$$v \cos \varphi = \sum_n C_n^0 \bar{P}_n^0 + 2 \sum_{m,n} \bar{P}_n^m \left[C_n^{mc} \cos(m\psi) + C_n^{ms} \sin(m\psi) \right] \quad (44)$$

Notice that, for axial flow, the advance ratio (μ) is zero. For an ideal actuator disk, the non-dimensional climb rate (λ) is arbitrarily small, whereas for tilted lift it will have a finite value.

From He's inflow equations (10) and (11) for an infinite number of blades, this is a steady system. Furthermore, all the coefficients associated with the sine component are zero, that is, β^m and τ^{ms} are zero.

Rearranging the equation with this in mind, it can be solved in matrix form for the induced velocity coefficients, as expressed by:

$$V[\tilde{L}^c]^{-1}\{\alpha_n^m\} = \frac{1}{2}\{\tau_n^{mc}\} \quad (45)$$

$$\{\alpha_n^m\} = \frac{1}{2V}[\tilde{L}_{nj}^{mr}]^{-1}\{\tau_j^r\} \quad (46)$$

Let the matrix \tilde{L} with the $m = 0$ row partition multiplied by two will be called $\bar{\bar{L}}$. Then, the minimum induced power problem can be formulated as the optimization of a functional J , shown, subject to the constraint expressed by Equation (48). The optimization is carried out in to yield the optimum value for the pressure coefficients.

$$J = \frac{1}{2} \frac{1}{V} \{\tau_n^m\}^T [\bar{\bar{L}}_{nj}^{mr}] \{\tau_j^r\} \quad (47)$$

$$\{\tau_n^m\}^T \{C_n^m\} = \frac{\sqrt{3}}{2} C_T \quad (48)$$

$$\delta [J - \Lambda \{\tau_n^m\}^T \{C_n^m\}] = 0 \quad (49)$$

$$\frac{1}{V} \left[\frac{1}{2} [\bar{\bar{L}}_{nj}^{mr}] + \frac{1}{2} [\bar{\bar{L}}_{nj}^{mr}]^T \right] \{\tau_n^m\} = \{C_n^m\} \Lambda \quad (50)$$

$$\{\tau_n^m\}_{optimal} = V \left[\frac{1}{2} [\bar{\bar{L}}_{nj}^{mr}] + \frac{1}{2} [\bar{\bar{L}}_{nj}^{mr}]^T \right]^{-1} \{C_n^m\} \Lambda \quad (51)$$

Equation (51) is the solution for this optimization problem, which will yield the minimum induced power for a lightly loaded actuator disk with infinite number of blades. In these equations Λ is the Lagrange multiplier of the optimization, that is chosen to give $\tau_1^0 = \sqrt{3}/2 C_T$, as it was explained for the constraint in the general formulation of an optimization process.

The general solution for the pressure coefficients can be applied to different cases. It is the purpose of this paper to show results for axial flow, but these coefficients can be also used to obtain pressure, circulation and inflow velocity for a variety of flows, including edgewise flow ($\chi = 90^\circ$). For axial flow, $\chi = 0^\circ$, the elements in $\bar{\bar{L}}$ are zero except when $r = m$.

With the calculation of thrust and power coefficients, the determination of the figure of merit is simple. The general solution for the figure of merit that will be shown by the use of finite-state methods is:

$$K = F.M._{finite-state} = 2 \{C_n^m\}^T [\bar{\bar{L}}]^{-1} \{C_n^m\} \quad (52)$$

The conditions for each of the special cases will cause the coefficient vector or the L-matrix to change, but the general form will remain for all of the cases.

Special Case of Actuator Disk

For the case of an actuator disk Equation (43) reduces to the unity ($\lambda = 0$) and the coefficients in Equations 40 through 42 reduce to:

$$C_1^0 = \int_0^1 \sqrt{3} v dv = \frac{1}{\sqrt{3}}$$

and all the others become:

$$C_n^m = 0$$

Therefore, the vector $\{C_n^m\}$ is the vector $\{1 \ 0 \ 0 \ \dots \ 0\}^T$ with as many elements as the number of terms that correspond to the harmonics studied in the problem and the optimization becomes simplified.

Momentum theory [5],[6] predicts that the minimum induced power for an actuator disk in axial flow will be achieved by constant pressure and constant inflow distributions. Results using the finite-state method show agreement with these predictions. Figures 7 and 8 show the constant profile for the pressure and the inflow respectively with a reduced amount of terms in the Fourier series. According to Momentum theory the lift distribution corresponding to this pressure and velocity should be linear. Finite-state methods agree with the predicted results, as it is shown in Figure 9.

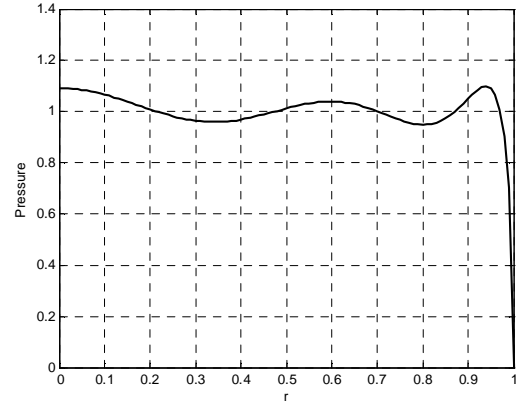


Figure 7: Pressure profile that provides minimum induced power for an actuator disk in axial flow with an infinite number of blades.

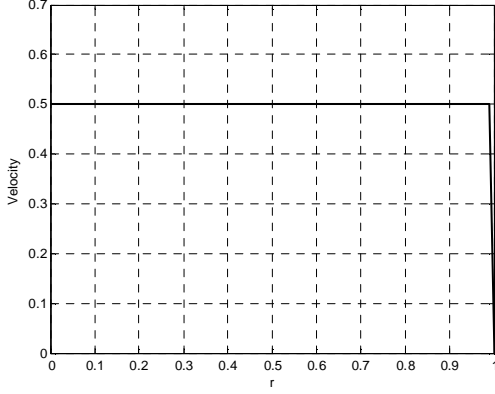


Figure 8: Velocity profile that provides minimum induced power for an actuator disk in axial flow with an infinite number of blades.

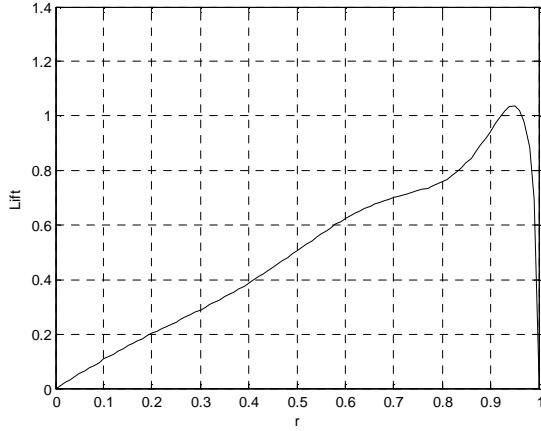


Figure 9: Lift distribution for optimum flow for an actuator disk with an infinite number of blades.

Closed-Form Expression.

Since the above shows that a formal optimization with the dynamic wake model gives the Glauert result for minimum power, it seems that it would be useful to consider some closed-form results under the Glauert hypothesis. From momentum theory [5],[6], one can show that

$$C_T = 2(\eta + \nu)v \quad (53)$$

$$C_p = 2(\eta + \nu)^2 v = (\eta + \nu)C_T \quad (54)$$

Because we optimize for a given C_T , it is very convenient to normalize all velocities on induced flow in hover.

Thus, $\bar{\eta} = \eta / \sqrt{C_T/2}$, $\bar{\nu} = \nu / \sqrt{C_T/2}$, $\bar{\lambda} = \bar{\eta} + \bar{\nu}$. It follows that the proper normalization of induced power is

$$\bar{C}_p = \frac{\sqrt{2}C_p}{C_T^{3/2}} \quad (55)$$

The result is a normalized set of inflow equations. The thrust equation becomes:

$$1 = (\bar{\eta} + \bar{\nu})\bar{\nu} \quad (56)$$

which can be solved for normalized or flow due to a normalized climb rate. That value can then be used to determine the normalized induced power for an ideal actuator-disk rotor.

$$\bar{C}_{p_i} = \bar{C}_p - \bar{\eta} = \left[\frac{\bar{\eta}}{2} + \left(\frac{\bar{\eta}^2}{4} + 1 \right)^{1/2} \right]^{-1} \quad (57)$$

One can see that the ideal induced power ranges from a normalized value of unity in hover ($\bar{\eta} = 0$) and then decreases with climb rate as $1/\bar{\eta}$. This is the Glauert result. We will use this ideal value to compare minimum power settings for various rotors. We will define a generalized figure of merit which is the ideal power, Equation (52), divided by the actual induced power.

Special Case of Lifting Rotor with an Infinite Number of Blades.

When the lift vector is tilted perpendicular to the vortex sheets, the ideal power is no longer attainable. Thus, uniform flow is no longer the optimum condition. Betz [7] determined that the minimum power is obtained when the induced flow at the individual blades is such that the vortex sheet remains along a helical path. Thus, the optimum inflow distribution is proportional to $\cos\phi$, Figure 5. For an infinite number of blades, it follows that the pressure field must follow this same shape. Thus, let the optimum pressure at the rotor be:

$$\Delta P = \frac{\Lambda V}{2} \cos\phi = \frac{\Lambda V}{2} \frac{r}{\sqrt{r^2 + \lambda^2}} \quad (58)$$

where k is a Lagrange multiplier. Then the induced velocity, w is:

$$w = \frac{1}{2V} \Delta P = \frac{\Lambda}{4} \frac{r}{\sqrt{r^2 + \lambda^2}} \quad (59)$$

The thrust coefficient is :

$$C_T = 2 \int_0^1 \Delta P \cos\phi r dr = \Lambda V \int_0^1 \frac{r^3}{r^2 + \lambda^2} dr \quad (60)$$

dividing both sides by C_T , introducing the normalized values $\bar{\Lambda} = \frac{\Lambda}{\sqrt{C_T/2}}$ and $\bar{V} = \frac{V}{\sqrt{C_T/2}}$, and letting

$y \equiv r/\lambda$ we obtain an expression that can be integrated to obtain a solution in closed form.

$$1 = \frac{\bar{\Lambda}\bar{V}}{2} \lambda^2 \int_0^{1/\lambda} \frac{y^3}{1+y^3} dy \quad (61)$$

performing the integration on Equation (61) gives the value of the normalized Lagrange multiplier to be:

$$\bar{\Lambda} = \frac{4}{\bar{V}} \frac{1}{1 - \lambda^2 \ln\left(1 + \frac{1}{\lambda^2}\right)} \quad (62)$$

To obtain the induced power coefficient, we must consider the power.

$$C_p = 2 \int_0^1 \Delta P_w r dr = \frac{\Lambda^2 V}{4} \int_0^1 \frac{r^3}{r^2 + \lambda^2} dr \quad (63)$$

Then, the normalized power coefficient is:

$$\bar{C}_{p_i} = \frac{C_p}{2(C_T/2)^{3/2}}, \text{ which provides the final expression}$$

for the normalized induced power.

$$\bar{C}_{p_i} = \frac{\bar{\Lambda}}{4} = \frac{1}{\bar{V}} \frac{1}{1 - \lambda^2 \ln\left(1 + \frac{1}{\lambda^2}\right)} \quad (64)$$

$$\text{For axial flow, } \bar{V} = \bar{\lambda} = \bar{\eta} + \bar{v} = \frac{\bar{\eta}}{2} + \sqrt{\frac{\bar{\eta}^2}{4} + 1}.$$

The result of this closed-form solution yields the expression for the ideal figure of merit for a lifting rotor with an infinite number of blades. Rearranging the previous equations, one obtains:

$$K = F.M._{Betz} = 1 - \lambda^2 \ln\left(1 + \frac{1}{\lambda^2}\right) \quad (65)$$

The question remains if the use of finite-state methods will suffice to obtain the Betz distribution for a lifting rotor with an infinite number of blades. To verify this, the figure of merit is found by finite-state methods using the formulation described in the optimization section. These coefficients represent the general solution. To customize them to the present special case, some modifications were performed. Since the present cases are for axial flow, the matrix $\left[\bar{L}\right]$ — defined by Equation

(13) — simplifies to a diagonal in terms of Γ_{jn}^{mm} . It should

be noted that these matrices are identical to $\left[A_{nj}^m\right]$ in Ref.

3. For an infinite number of blades in axial flow, $C_n^m = 0$ except when $m = 0$ so that only A_{jn}^0 enters the optimization. C_n^0 comes from the following integral over the wake skew angle,

$$C_n^0 = \frac{1}{2\pi} \int_0^{2\pi} \int_0^1 \cos \varphi \bar{P}_n^0(v) v dv d\psi$$

where $\cos \varphi = \frac{r}{\sqrt{r^2 + \lambda^2}}$ and $r dr = -v dv$. With those C_n

the thrust and power coefficients become:

$$C_T = 2 \sum_{n=1,3,5} C_n \tau_n^{0c} \quad (66)$$

$$C_p = \eta C_T + \sum_{n=1,3,5} 2\alpha_n^0 \tau_n^{0c} \quad (67)$$

For this optimization, again the power coefficient is minimized for constant thrust, and the functional J becomes:

$$J = \eta C_T + \sum_{n=1,3,5,\dots} \frac{1}{2V} \{\tau_n^{0c}\}^T \left[A_{nj}^0\right] \{\tau_j^{0c}\} - \Lambda \sum_{n=1,3,5,\dots} C_n \tau_n^{0c} \quad (68)$$

where Λ is the Lagrange multiplier. Performing the optimization ($\delta J = 0$), the optimal pressure coefficients for this particular case are:

$$\{\tau_j^{0c}\}_{optimal} = \left[A_{nj}^0\right]^{-1} \{C_n\} \Lambda V \quad (69)$$

Introducing the above changes to the general optimization formulation, the figure of merit using finite-state methods is:

$$F.M._{finite-state} = 2 \{C_n\}^T \left[A_{nj}^0\right]^{-1} \{C_n\} \quad (70)$$

Figure 10 shows the comparison for the figure of merit from the finite-state method as compared to the Betz formula. It is seen that the finite-state method agrees satisfactorily with Betz result. The difference between them can be reduced by addition of more terms to $\left[A_{nj}^0\right]$ and $\{C_n\}$. However, the present approximation, which uses twenty terms is thought to be close enough so that the dynamic inflow model is verified.

What is most important about Figure 10 is the large drop in figure of merit with climb rate, even for an optimized rotor. The drop is due purely to the effects of tilted lift and swirl velocity. It may well be that the deficiency in rotor efficiency in forward flight is due to a similar phenomenon.

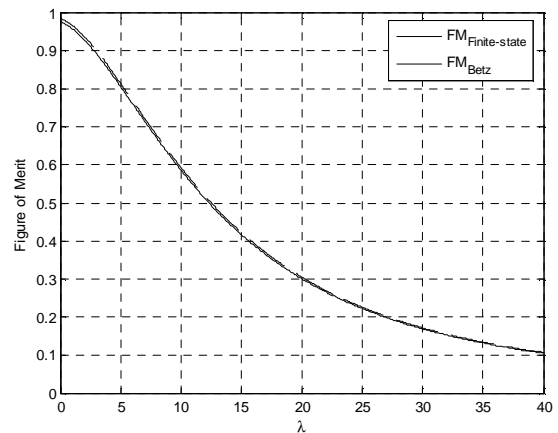


Figure 10: Comparison of the finite-state optimization to Betz distribution.

Figure 11 gives Figure of Merit as a function of climb rate η rather than λ . Since λ is determined by the total flow through the rotor, the Figure of Merit thus becomes a

function both of climb rate η and thrust coefficient C_T . For larger climb rate, the effect of C_T is diminished.

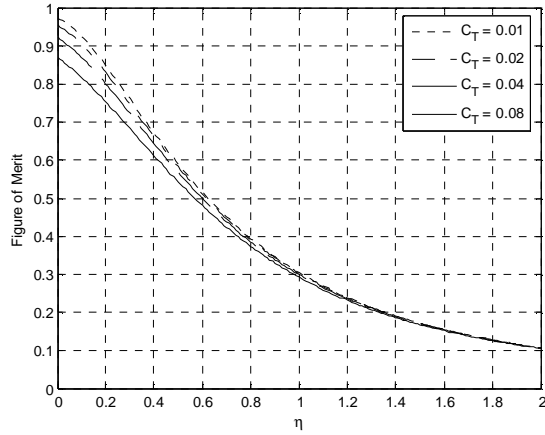


Figure 11: Figure of Merit versus climb rate for different thrust coefficients (infinite number of blades).

Figure 12 presents the induced power coefficient as a function of climb rate for a range of C_T values.

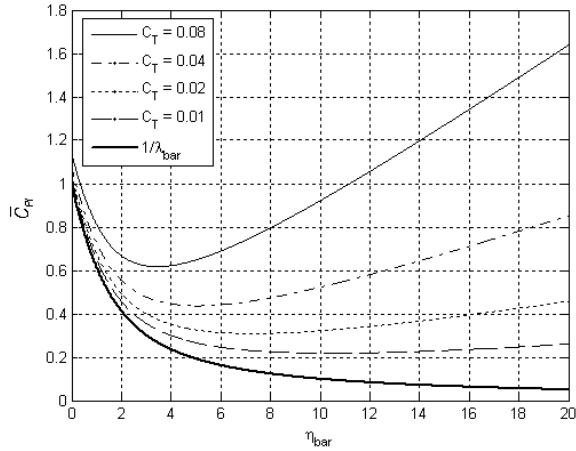


Figure 12: Induced power coefficient (helicopter convention) versus climb rate (infinite number of blades)

An important characteristic seen in Figure 12 is a “bucket” in the induced power for each thrust coefficient at a given climb rate. This is due to the fact that ideal power decreases with η whereas the figure of merit also decreases with η . Thus, there is an optimum climb rate. The lowest curve is for $C_T = 0$ and is equal to $1/\lambda_{bar}$. This

ideal minimum power monotonically decreases with $\bar{\eta}$, so the “bucket” is not present, and the induced power coefficient does not increase for high climb rates.

Special Case of Finite Number of Blades.

The effect of a finite number of blades is a further loss in wake energy due to the individual vortex sheets from each blade. Goldstein worked out the exact effect for optimized rotors. Prandtl, on the other hand, worked out an approximate correction factor that agrees very well with Goldstein for moderate climb rates. Prandtl [5],[6],[7] introduces a correction factor, k , in the calculation of induced flow that accounts for the loss at the tip of the blades. Because of this tip loss, for a given thrust, there is more induced flow than predicted by momentum theory. Using these principles an approximation to the theoretical figure of merit for an actuator disk or a lifting rotor for a finite number of blades can be obtained using Prandtl formulation. The Prandtl k factor is applied as follows.

$$dL = (2\pi r dr) \rho (V + v)(2v)k \quad (71)$$

where

$$k = \frac{2}{\pi} \cos^{-1} \left[\exp \left(\frac{-Q(1-r)}{2\lambda} \right) \right] \quad (72)$$

where Q is the number of blades.

Because the Prandtl correction as applied to the Betz distribution agrees so closely with Goldstein, that it makes sense to do some calculations with the Prandtl factor to determine the magnitude of the effect of number of blades on figure of merit. Thus, the following formula can be used for the figure of merit computations.

$$K = F.M._{Prandtl} = 2 \int_0^1 k \cos^2 \varphi dr \quad (73)$$

where,

$$\cos \varphi = \frac{r}{\sqrt{r^2 + \lambda^2}} \quad (74)$$

where λ is the climb rate and φ is the inflow angle.

Figure (13) shows the effect of tip loss (as determined from Prandtl’s k -factor) on Figure of Merit. The top curve, for the case $\varphi = 0$, is the effect for an actuator disk with a finite number of blades for a four-bladed, lightly loaded rotor. The middle two, coincident curves are the figure of merit for a rotor with tilted lift but infinite number of blades. The lowest curve is for tilted lift and finite number of blades (i.e., the Goldstein solution). One can see that blade number is also an important factor in the loss of ideal induced power.

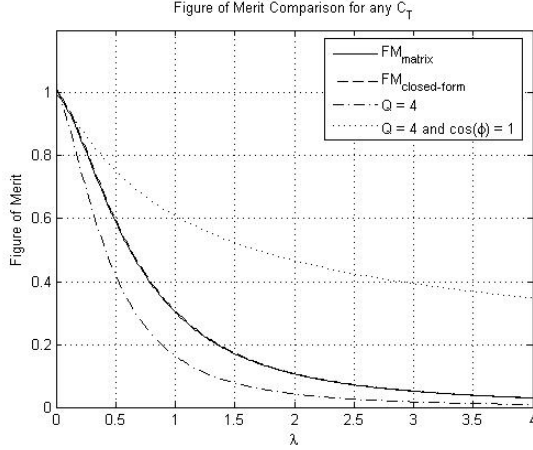


Figure 13: Effect of Tip Loss on Figure of Merit, Lightly-Loaded Rotor.

We now wish to see if the finite-state methodology can give the correct optimum distribution and figure of merit as Goldstein (i.e., as the Prandtl-corrected Betz). Makinen, [8],[9] showed that the inflow model can indeed match Goldstein provided that a correction is applied for the swirl kinetic energy. Thus, the added energy is added to the mass matrix; and the resultant induced flow is assumed parallel to the tilted lift vectors.

To be precise, the apparent mass matrix $[K_n^m]$ (diagonal), must be replaced to include the effect of the wake swirl. There are different swirl corrections that can be applied, but from Ref. 8 the following correction gives the best results.

$$[K_n^m] \Rightarrow [\sqrt{K_n^m}] \left[[I] + m \left(\frac{\kappa \lambda}{Q} \right)^2 \left[[I] - [A_{nj}^m]^2 \right]^{-m} \right] [\sqrt{K_n^m}] \quad (75)$$

where $\kappa = 2.2$, Q is the number of blades, and λ is the total inflow. It should be noted that for an actuator disk (no lift tilt), κ is set to zero.

When the dynamics of the unsteady blade-passage is added to the dynamic wake model, (see Ref. 8) shows that the \tilde{L} used in axial flow, $[A_{nj}^0]$, is replaced by the following.

$$\begin{aligned} [\tilde{L}] = & [A_{nj}^0] + \\ & 2 \sum_{m=Q, 2Q, 3Q, \dots} [E_{nj}^{m0}]^T [A_{nj}^m]^{-1} \\ & + \left(\frac{m}{\lambda} \right)^2 [K_n^m] [A_{nj}^m] [K_n^m]^{-1} [E_{nj}^{m0}] \end{aligned} \quad (76)$$

The $[E_{nj}^{m0}]$ matrix is the expansion transformation matrix (Ref. 8) defined as:

$$E_{nj}^{m0} = \int_0^1 \bar{P}_n^m(v) \bar{P}_j^0(v) dv \quad (77)$$

Performing the optimization for this case, and using finite-state methods, the figure of merit is obtained. The $\{C_n^m\}$ remains the same as for an infinite number of blades. There is no change in the values because physically these coefficients are a fit of the function $v \cos \phi$, and for an actuator disk $\cos \phi = 1$.

$$K = F.M._{finite-state} = 2 \{C_n^m\}^T [\tilde{L}]^{-1} \{C_n^m\} \quad (78)$$

Once the theory has been verified, some useful plots of induced power for different numbers of blades at various climb rates can be obtained, as it is shown in Figure 14. The importance of this graph is that the effect of finite number of blades on the induced power can be noticed. It is seen that induced power increases for a decreasing number of blades. It is an expected result, as the ideal induced power exists for an infinite number of blades (for Prandtl is $k = 1$). The profile of the curves is similar to the one observed for infinite numbers of blades at different thrust coefficients. The “bucket” effect is present here also, and the general profile is maintained. Thus, the effect of these differences for finite number of blades affecting the induced power is as less critical as the increase in induced power due to lift tilt.

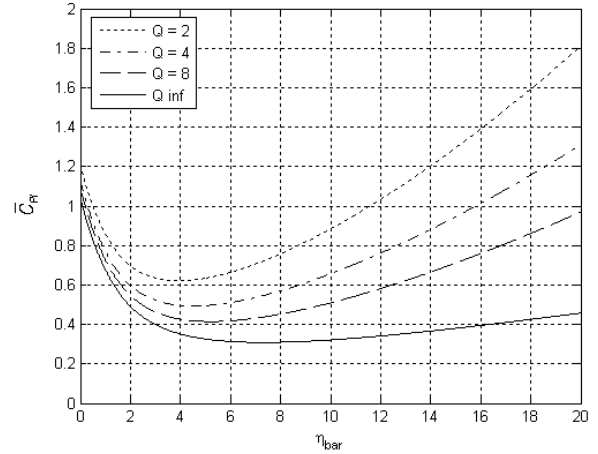


Figure 14: Induced power coefficient comparison for various numbers of blades. $C_T = 0.02$.

Finite-State methods should agree with the theory developed by Goldstein [10] for every flight condition in axial flow. There is no closed-form solution or expression that Goldstein developed for the theoretical figure of merit for a lifting rotor with a finite number of blades. However, Makinen [8],[9] was successful in the further development and application of the finite-state method to obtain circulation for a given induced velocity. These circulation results are in agreement with

Goldstein's circulation for an optimal propeller, as it is shown in Figures 15 and 16. The fact that the application of finite-state methods provides an accurate optimal circulation results in the confidence that the calculations of figure of merit for this special case will also be accurate.

Figures 15 and 16 show the circulation at any radial location of the blade using Prandtl's approximation, Goldstein's optimal circulation, and Makinen's results with the swirl velocity corrections made to the apparent mass matrix in Equation (75). Figure 15 is for a $\mu_0 = 5$ ($\lambda = 0.20$) and Figure 16 is for $\mu_0 = 20$ ($\lambda = 0.05$). It is noticed that Prandtl and Goldstein's circulations give results that are very close to each other. Since there is such close agreement in both approaches, and there is a figure of merit expression for Prandtl's approximation, the finite-state approach could be compared to Prandtl's approximation.

It is not surprising that the quadratic optimization with the dynamic wake model gives the correct figure of merit due to both lift tilt and finite number of blades. Figures 15 and 16 (from Ref. 8) show that the dynamic wake model (with swirl correction) gives the correct inboard (swirl) and outboard (tip loss) velocities.

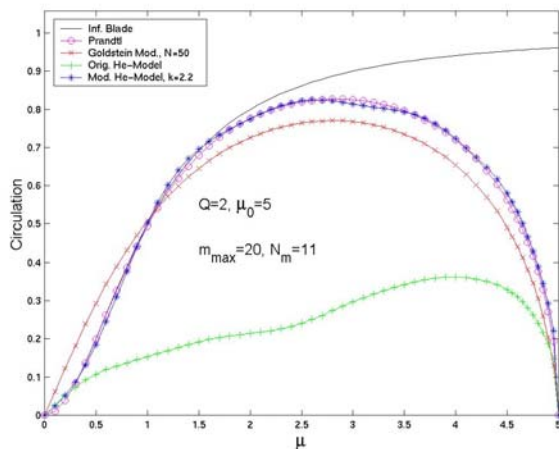


Figure 15: Circulation at any blade radial location for Prandtl, Goldstein, and using Finite-State methods. Plot obtained from [8],[9].

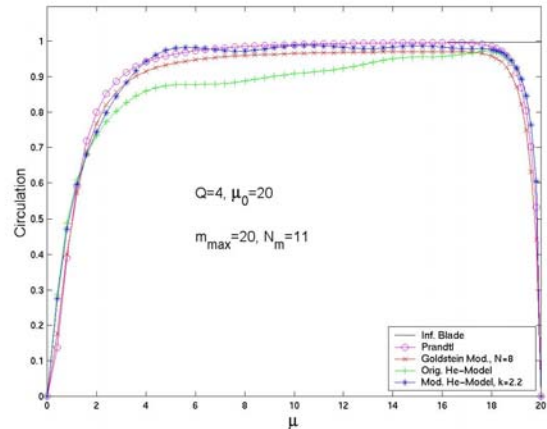


Figure 16: Circulation at any blade radial location for Prandtl, Goldstein, and using Finite-State methods. Plot obtained from [8],[9].

Future Work

Since the method has been validated, the theory can be applied to the same cases for skewed flow. Most of the approach for skewed flow is similar to that for axial flow. The case for an actuator disk with an infinite number of blades will be revisited. However some changes will be done for forward flight. For this case, momentum theory predicts that the optimum induced power is obtained for a constant pressure distribution (similarly as to what happened for axial flow) but the induced velocity profile will no longer be constant. For an actuator disk with an infinite number of blades, we have already applied the finite-state model and verified that it gives the Glauert solution of uniform pressure. However, to go on to the other cases, all harmonics (and their periodic coupling) will need to be included. The rest of the special cases, for an actuator disk with a finite number of blades and for the two cases for a lifting rotor, will provide results never obtained before. The results will hopefully provide the conclusion as to why the experimental minimum induced power for a helicopter is orders of magnitude greater to what theory predicts should be. These results could allow determining what changes, if any, should be introduced in the rotor to reduce the minimum induced power.

The formulation for the figure of merit in forward flight will remain similar to the general figure of merit shown by Equation (52):

$$K = F.M._{finite-state} = 2 \{C_n^m\}^T \left[\bar{L} \right]^{-1} \{C_n^m\}$$

However, the coefficients and the L-matrix will be different than the ones obtained before, and also different for each of the four cases.

The main difference for skewed flow is that when calculating the cosine of the inflow angle the advance ratio, μ , must be considered. Equation (43) again is:

$$\cos \varphi = \frac{r + \mu \sin \psi}{\sqrt{(r + \mu \sin \psi)^2 + \lambda^2}}$$

where r is the radial position along the blade and ψ is the angle at which the rotating blade is with respect to the aft position of the rotor.

For skewed flow, the total inflow also changes. The total inflow for axial flow was defined before as:

$$\bar{\lambda} = \bar{\eta} + \bar{v} = \frac{\bar{\eta}}{2} + \sqrt{\frac{\bar{\eta}^2}{4} + 1}$$

and it was derived from momentum theory for a uniform induced flow distribution. In forward flight, the total inflow becomes:

$$\bar{\lambda} = \bar{\eta} + \bar{v} \quad (79)$$

where the normalized inflow is the solution of Equation (80) for given normalized climb rate and advance ratio.

$$1 = \bar{v} \sqrt{\bar{\mu}^2 + (\bar{v} + \bar{\eta})^2} \quad (80)$$

These changes will affect the optimum coefficients, but the L-matrix will also be altered because the skew angle is no longer zero, and so there are more harmonics than the $m = 0$ for axial flow. The expression for this matrix will be obtained using He's formulation (Equations (13)).

With the results in forward flight, the study of minimum induced power will be complete for any flight condition.

Conclusions

The objective of this paper is to validate the use of finite-state methods to obtain accurate minimum induced power results. The theory is validated by the comparison to classical solutions for the figure of merit. The results compare favorably for a variety of flight regimes in axial flow. The current method was verified for: 1) an actuator disk with an infinite number of blades, which was in agreement with the predictions made by momentum theory; 2) for an actuator disk with a finite number of blades, which proves similar results as to the ones obtained by Prandtl; 3) for a lifting rotor with an infinite number of blades, which agrees with Betz's distribution; and 4) for a lifting rotor with a finite number of blades, which should agree with Goldstein's solution, but was compared to Prandtl's approximation modified to include a finite number of blades.

Because the method has been validated for all the cases in axial flow, it is hopeful that the formulation can

be used to obtain results for skewed flow in all four special cases. These will result in the fulfillment of the complete scope of flight conditions for a helicopter, and will provide a greater understanding on what the requirements are for minimum induced power conditions.

Also, because of the results obtained by Ormiston [1],[2], a conclusion as to what makes the induced power to increase well above ideal values should be found. These studies will determine which of the three main causes for the increment of induced power is the most important: the fact that a real rotor has a finite number of blades, the limitations in lifting capabilities of the blades as airfoils, or the tilted thrust that produces swirl velocity.

Acknowledgements

This work was sponsored by the Army Research Office, Agreement #DAAD19-01-1-0697, Tom Doligalski, Technical Monitor.

References

- Ormiston, Robert A., "Helicopter Rotor Induced Power," Proceedings of the AHS International 60th Annual Forum and Technology Display, Baltimore, MD, June 8-10, 2004.
- Ormiston, Robert A., "Further Investigations of Helicopter Rotor Induced Power," Proceedings of the AHS International 61st Annual Forum and Technology Display, Grapevine, TX, June 1-3, 2005.
- Chengjian, He, *Development and Application of a Generalized Dynamic Wake Theory for Lifting Rotors*, Ph.D. thesis, Georgia Institute of Technology, July 1989.
- Glauert, H., *Aerodynamic Theory: A General Review of Progress*, volume IV, chapter Division L, Airplane Propellers. Dover Publications, Inc., New York, NY, 1963, pp. 169-368
- Gessow, A. and Myers, Garry C., *Aerodynamics of the Helicopter*, Ungar, New York, 1952.
- Johnson Wayne, *Helicopter Theory*, Dover Publications, Inc., New York, NY, 1980.
- Betz, A., and Prandtl, L., "Schraubenpropeller mit geringstem energieverlust," Goettinger Nachrichten, March 1919, pp. 193-217
- Peters, D.A., and Makinen, SM., "A Comparison of Prandtl and Goldstein Optimum Propeller Solutions with Finite-State Dynamic Wake Models," Georgia Institute of Technology and Army Research Office 10th International Workshop on Aerolasticity of Rotorcraft Systems, Atlanta, GA, November 3-5, 2003.

9. Makinen, S.M., “Applying Dynamic Wake Models to Large Swirl Velocities for Optimal Propellers, ” Doctoral thesis, Washington University in Saint Louis, May 2005.

10. Goldstein, S., “On the Vortex Theory of Screw Propellers,” Proceedings of the Royal Society of London. Series A, Containing Papers of a Mathematical and Physical Character, volume 123. The Royal Society, April 6 1929, pp. 440-465

Addendum

Equations (52), (65), (73), and (78) give formulae for Figure of Merit for a lightly-loaded rotor. Thus, to be precise, they are actually formulae for thrust deficiency K. This thrust deficiency is a function of λ , the flow rate. In order to extend these formulae to apply to rotors with significant loading (i.e., v not small relative to η) one must correct for the lift deficiency in the momentum equation (54). This is done as follows.

First, λ is computed without thrust deficiency

$$\lambda = \frac{\eta}{2} + \sqrt{\left(\frac{\eta}{2}\right)^2 + \frac{C_T}{2}}$$

and this λ is used to compute the thrust deficiency K. Next, K is used in the momentum theory to compute Figure of Merit.

$$F.M. |_{\text{lightly-loaded}} = \frac{K \left[\frac{\eta}{2} + \sqrt{\left(\frac{\eta}{2}\right)^2 + \frac{C_T}{2}} \right]}{\left[\frac{\eta}{2} + \sqrt{\left(\frac{\eta}{2}\right)^2 + \frac{C_T}{2K}} \right]} \quad (81)$$

For lightly loaded, $\eta^2 \gg 2C_T$, this reverts to F.M. = K.
For hover, $\eta = 0$, this reduces to

$$F.M. |_{\text{hover}} = K^{3/2}$$

Thus, Equation (81) is the Figure of Merit for full loading.